

The non-reciprocal Ising model

Yael Avni,¹ Michel Fruchart,² David Martin,³ Daniel Seara,¹ and Vincenzo Vitelli^{1,4}

¹University of Chicago, James Franck Institute, 929 E 57th Street, Chicago, IL 60637

²Gulliver, ESPCI Paris, Université PSL, CNRS, 75005 Paris, France

³University of Chicago, Kadanoff Center for Theoretical Physics and Enrico Fermi Institute, 933 E 56th St, Chicago, IL 60637

⁴University of Chicago, Kadanoff Center for Theoretical Physics, 933 E 56th St, Chicago, IL 60637

Systems with non-reciprocal interactions generically display time-dependent states. These are routinely observed in finite systems, from neuroscience to active matter, in which globally ordered oscillations exist. However, the stability of these uniform non-reciprocal phases in noisy spatially-extended systems, their fate in the thermodynamic limit, and the criticality of the corresponding phase transitions are not fully understood. Here, we address these questions by introducing a non-reciprocal generalization of the Ising model and study its critical behavior by means of numerical and analytical approaches. While the mean-field equations predict three stable homogeneous phases (disordered, ordered and a time-dependent swap phase), our large scale numerical simulations reveal a more complex picture. Static order is destroyed in any finite dimension due to the growth of rare droplets unless the symmetry between the two spins types is broken triggering a stabilizing droplet-capture mechanism. The swap phase is destroyed by fluctuations in two dimensions through the proliferation of spiral defects, but stabilized in three dimensions where non-reciprocity changes the critical exponents from Ising to XY, thus giving rise to a robust spatially-distributed clock.

Non-reciprocal interactions naturally arise in out-of-equilibrium systems [1–22] ranging from neuroscience [23–25] and social networks [26, 27] to ecology [28–30] and open quantum systems [31–33]. A generic feature of these systems is the emergence of many-body limit cycles – time-dependent states arising from non-mutual interactions between constituents. Such states are routinely observed in experiments and simulations of finite systems. A single limit cycle oscillator subject to noise eventually forgets the initial phase [34–44]: its temporal correlations decay with time very much like density fluctuations decay with spatial separation in a liquid (Fig. 1a, left). In many-body systems, however, coherent oscillations may be restored over arbitrarily long periods [45–64]: temporal correlations persist (without any periodic drive externally imposing a phase) very much like spatial correlations do in a crystal (Fig. 1a, right). In this Letter, we ask: Can many-body limit cycles survive fluctuations in spatially-extended, locally-coupled non-reciprocal systems of arbitrary size? If so, what are the critical exponents of the resulting phase transitions? We address these questions by introducing a non-reciprocal generalization of what is perhaps the most paradigmatic statistical mechanical system: the Ising model.

Dynamics without global optimisation.— In equilibrium, the dynamics of Ising spins is described by kinetic Ising models in which spins $\sigma_n = \pm 1$ tend to minimize a global potential, and hence interact reciprocally [65, 66]. To account for non-reciprocal interactions, we instead assume that each spin σ_n tends to minimize its own *selfish energy* E_n , and choose the probability of flipping σ_n at each time step to be given by the Glauber rule

$$p(\sigma_n \rightarrow -\sigma_n) = \frac{1}{2} [1 - \tanh(\Delta E_n / (2k_B T))] \quad (1)$$

where ΔE_n is the change in selfish energy between both

configurations, T is the temperature, and k_B the Boltzmann constant. Since we define different potential functions for each spin, the dynamics cannot be derived from a single potential function and detailed balance is broken. This formulation encompasses several non-reciprocal dynamics used among the physical sciences [67–76].

The non-reciprocal Ising model.— Systems with non-reciprocal couplings do not always exhibit macroscopic oscillations. These tend to occur, when a small number of species have competing goals. Correspondingly, we split the spins $\sigma_n \equiv \sigma_i^\alpha$ into two species, labeled by Greek indices $\alpha = A, B$, located on sites i of a d -dimensional cubic lattice of linear size L (Fig. 1b). Spins of the same species tend to align with their neighbors, while spins of different species interact in a non-reciprocal manner: spins A tend to align with spins B , whereas spins B tend to anti-align with spins A . This is captured by the selfish energy

$$E_i^\alpha = -J \sum_{j \text{ nn of } i} \sigma_i^\alpha \sigma_j^\alpha - K \varepsilon_{\alpha\beta} \sigma_i^\alpha \sigma_i^\beta \quad (2)$$

with $J, K > 0$, where the first term captures the *intra-species* interactions with the sum running over nearest neighbors of i , and the second term captures the *inter-species* interactions where summation over species indices β is implied ($\varepsilon_{\alpha\beta}$ is the Levi-Civita symbol). We have assumed for simplicity that inter-species interactions only occur on-site and are purely non-reciprocal (reciprocal on-site interactions are considered in [77]).

Mean-field equation.— Within the mean-field approximation and upon rescaling of time and space, the dynamics of the average magnetization $m_\alpha(\vec{r}, t)$ is [77]

$$\partial_t m_\alpha = -m_\alpha + \tanh \left[\tilde{J} m_\alpha + \tilde{K} \varepsilon_{\alpha\beta} m_\beta + D \nabla^2 m_\alpha \right] \quad (3)$$

where $D \equiv J/(k_B T)$, $\tilde{K} = K/(k_B T)$ and $\tilde{J} \equiv 2dJ/(k_B T)$.

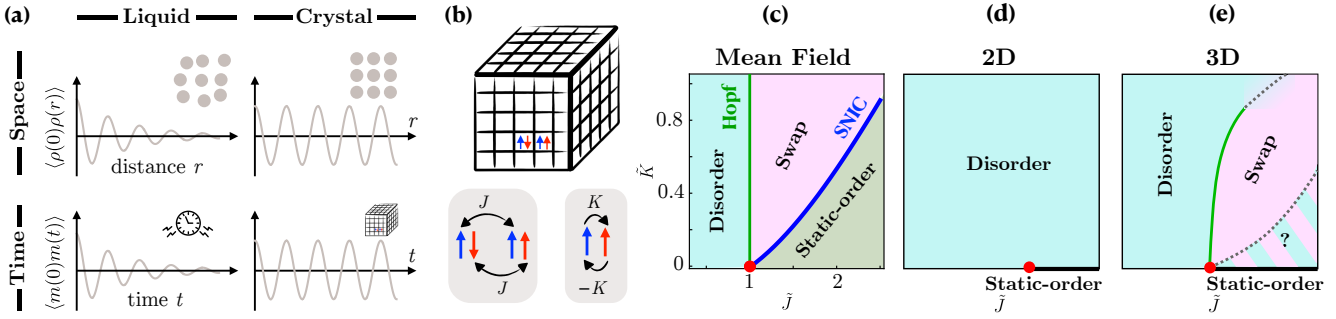


Fig. 1. Non-reciprocal Ising model. (a) Comparison of noisy (left) and robust (right) clocks with different types of spatial order. (b) Schematic drawing of the non-reciprocal Ising model. The model includes two species per site with two interaction types: 1) intra-species reciprocal nearest-neighbors interaction of strength J and 2) inter-species non-reciprocal on-site interaction of strength K . (c) Mean-field phase diagram, (d) schematic 2D phase diagram and (e) schematic 3D phase diagram. The three phases shown on the diagrams are (i) disorder, (ii) swap and (iii) static order. The lines separating the phases are Hopf bifurcation (thin green), SNIC bifurcation (thick blue) and two yet undetermined transition lines (dashed grey). Red dot is the Pitchfork bifurcation.

The phase diagram in Fig. 1c shows the stable homogeneous solutions of Eq. (3) as a function of the couplings \tilde{J} and \tilde{K} . When non-reciprocal interactions are turned off ($\tilde{K} = 0$), a pitchfork bifurcation at $\tilde{J}_c \equiv 1$ (red point in Fig. 1c) separates a disordered phase (in blue) from a ferromagnetic phase (in green), as in the equilibrium Ising model. When non-reciprocal interactions are present ($\tilde{K} \neq 0$), a time-dependent oscillatory state that we dub “swap phase” arises (in pink). This limit cycle state where both species flip their magnetizations repeatedly is separated from the disordered state by a Hopf bifurcation at $\tilde{J}_c = 1$ (green line), and from the ferromagnetic phase by another bifurcation known as a saddle-node on an invariant circle (SNIC) bifurcation [78, 79] (blue line). The shape of the limit cycle in (m_A, m_B) space evolves from a circle near the Hopf bifurcation to a square near the SNIC bifurcation [77]. The oscillation period remains finite at the Hopf bifurcation, and it diverges at the SNIC bifurcation [78].

Monte-Carlo simulations.— To go beyond the mean-field description, we perform large-scale Monte-Carlo (MC) simulations of the non-reciprocal Ising model in both two and three dimensions (see [77] for details on the update rules; we did not observe qualitative differences with other update rules). Unless mentioned otherwise, we initialize the system in an ordered state where all spins of the same species are either up or down, and let the system evolve until a steady-state is reached.

The qualitative results of our simulations are summarized in Fig. 1d-e. In 2D, any amount of non-reciprocity destroys all order. In 3D, our simulations suggest that the swap phase survives the thermodynamic limit, while the static ferromagnetic phase is eventually destroyed by any amount of non-reciprocity.

In order to distinguish the different possible phases, we

introduce the synchronization order parameter [45]

$$R \equiv \langle s \rangle_{t,\Omega} \quad \text{with} \quad s \equiv \frac{1}{L^d} \left| \sum_j e^{i\theta_j} \right| = \sqrt{\frac{M_A^2 + M_B^2}{2}} \quad (4)$$

and the phase space angular momentum [80]

$$\mathcal{L} \equiv \langle \ell \rangle_{t,\Omega} \quad \text{with} \quad \ell \equiv M_B \partial_t M_A - M_A \partial_t M_B \quad (5)$$

where θ_j is the angle on the (σ_j^A, σ_j^B) plane (Fig. 2a), $M_\alpha = \sum_j \sigma_j^\alpha / L^d$ are the total magnetizations and the average $\langle \dots \rangle_{t,\Omega}$ is over time and realizations. The synchronization order parameter R is zero if the system is disordered and nonzero in both the swap and static-order phases, while \mathcal{L} is zero in the disordered and static-order phases and non-zero in the swap phase.

Destruction of the swap phase in 2D by spiral defects.— In small 2D systems, simulations show states in which M_A and M_B oscillate in time (like in the mean-field swap phase) with a large amplitude. However, oscillations are irregular, and typically occur through nucleation of droplets of opposite magnetization by the “unsatisfied” species, in alternating order (see Movie 1). As the size L increases, it becomes apparent that this oscillatory state is a transient, eventually destabilized by proliferation of spiral defects similar to the rotational-symmetric spirals observed in the complex Ginzburg-Landau equation [47, 81–90], but whose shape has 4-fold rotational symmetry (four “arms”). This is evidenced in Fig. 2b-c, which shows the emergence of defects in the angle θ and the resulting drop in the magnetizations M_A and M_B after an oscillatory transient, along with snapshots of θ at different stages (see also Movie 1).

Quantitatively, the absence of a swap phase in the thermodynamic limit can be seen from the behavior of the order parameters as system size increases. Figure. 2d shows a color map of \mathcal{L} as a function of \tilde{J} and \tilde{K} . While a regime in which $\mathcal{L} \neq 0$, corresponding to the swap phase, appear

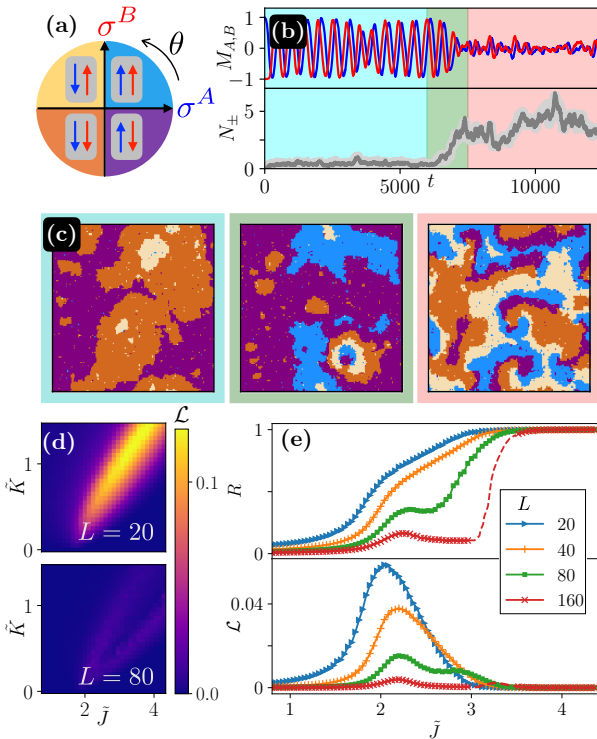


Fig. 2. Destruction of the swap phase by spiral defects in 2D. (a) Color code of the angle variable, θ . (b) The magnetizations (top) of species A (blue) and B (red) and the number of + and - defects (bottom) N_+ (dark grey) and N_- (bright grey) averaged over 100 time steps as a function of time. MC simulation parameters: $\tilde{J} = 2.8$, $\tilde{K} = 0.3$, and $L = 150$. We identify defects as adjacent 2 by 2 sites with a cycle of $\uparrow\uparrow\rightarrow\uparrow\downarrow\rightarrow\downarrow\downarrow\rightarrow\downarrow\uparrow$, either clockwise (+ defects) or anti-clockwise (- defects). (c) Snapshots of θ before (left), at the onset (middle), and after (right) the proliferation of spiral defects (frame color corresponds to colored regions in panel b). (d) Color map of phase space angular momentum, \mathcal{L} , as a function of \tilde{J} and \tilde{K} , for linear system size $L = 20$ (top) and $L = 80$ (bottom). (e) Synchronization order parameter R (top) and \mathcal{L} (bottom) as a function of \tilde{J} for $\tilde{K} = 0.3$ and different L . Dashed red line shows upper bound for R and \mathcal{L} for points that did not converge during simulation running time.

at $L = 20$, it almost diminishes completely at $L = 80$. A more thorough analysis is shown in Fig. 2e where both R and \mathcal{L} are shown as a function of \tilde{J} and fixed \tilde{K} for different system sizes. In the intermediate region corresponding to the swap phase ($1.5 \lesssim \tilde{J} \lesssim 3$), both R and \mathcal{L} go to zero as L increases, thereby indicating the destruction of the swap phase. In addition, the putative critical \tilde{J} marking the transition from disorder to swap depends on the system size, signifying the absence of a well-defined phase transition in the thermodynamic limit.

Existence of a stable swap phase in 3D and critical exponents.— In 3D, we find that a stable swap phase does exist. Its behavior is demonstrated in Fig. 3a where we show a kymograph of the θ -field of a single 1D row

in the 3D lattice as well as plot the total magnetizations as a function of time (see also Movie 2). The oscillations are spatially homogeneous and $M_A(t)$ and $M_B(t)$ have a fixed period and phase shift. The coherence time of M_A and M_B diverges with system size as $\tau_c \propto L^d$ (Fig. 3b), in agreement with a temporal crystal behavior (Fig. 1a) [91]. In the thermodynamic limit, coherent oscillations persist indefinitely despite the presence of noise.

Simulations with varying system sizes reveal a well-defined phase transition between a disordered phase with $R = 0$ to a swap phase with non-zero R . Figure 3d shows a color map of R in the (\tilde{K}, \tilde{J}) space, for $L = 320$, while Fig. 3e shows a cut of the color map for $\tilde{K} = 0.3$, for different L . Unlike in 2D (Fig. 2e), here there is a critical \tilde{J} , below which $R \sim L^{-d/2}$ and above which it converges to a non-zero value (Fig. 3e, inset). The stability of the swap phase in 3D holds even when the inter-species symmetry is broken by the addition of an on-site reciprocal coupling between the species, see Ref. [77].

Figure 3c shows that the phase-space trajectories become circular when approaching the phase transition line, supporting a Hopf behavior ([92]). Renormalization group studies based on the ϵ -expansion suggest that the field theory associated with the Hopf bifurcation in a spatially extended system has the same critical exponents as the XY model [93, 94]. Using finite-size scaling [77] and setting $\tilde{K} = 0.1$ we determine the critical exponents of the correlation length, susceptibility, and order parameter: $\nu = 0.68 \pm 0.02$, $\gamma = 1.33 \pm 0.04$, and $\beta = 0.35 \pm 0.01$, which are in good agreement with 3D XY critical exponents [95, 96], more so than with 3D Ising critical exponents [95] corresponding to the $\tilde{K} = 0$ case, see Fig. 3f.

For a fixed \tilde{K} , the critical \tilde{J} separating disorder from swap depends on \tilde{K} , in contrast with the mean-field prediction, in which \tilde{J}_c is independent of \tilde{K} (Fig. 1c). Above some critical \tilde{K} value, the phase transition loses its second-order-like nature (see $\tilde{K} \gtrsim 0.75$ region in Fig. 3d where R becomes discontinuous), apparently due to scroll waves (3D analog of spiral waves) [97–101] [77] that destabilize the swap phase. Within the size limitations of our simulations, it is unclear what part of the swap phase is destroyed by scroll waves in the thermodynamic limit and what type of phase transition is associated with their appearance (Fig. 1e).

We note that with random initial conditions, the system can coarsen into long-lived scroll waves and planar waves (Fig. 3g), even when ordered initial conditions would otherwise lead to global oscillations ([77] and Movie 3).

Stability of static-order phase and droplet growth in any finite dimension.— In finite systems, a ferromagnetic-like state with static order is observed both in 2D and 3D. As system size increases, however, this static state is destabilized by nucleation of droplets (see Fig. 4a and Movie 4) that grow and flip the magnetization, in alternating order of A- and B-spins. As a result, the static-order phase is replaced by droplet-induced os-

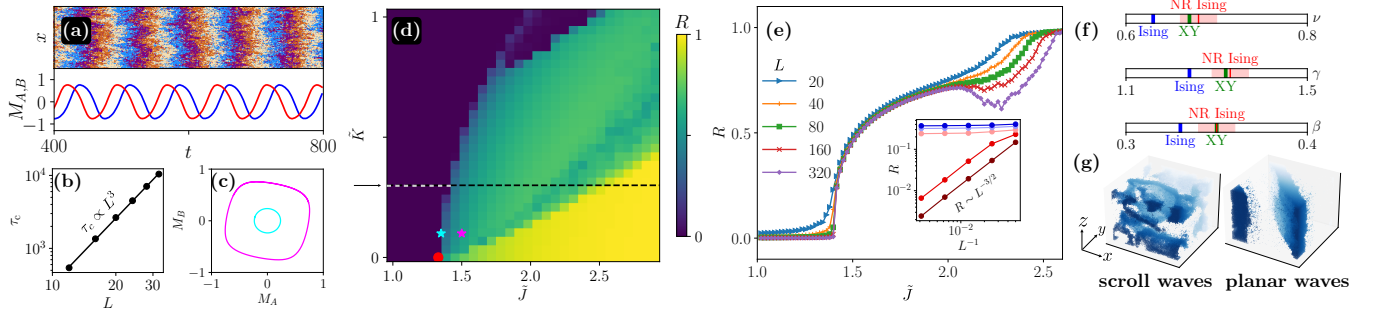


Fig. 3. Stability of the swap phase in 3D and critical exponents. (a) Time evolution of a stable swap phase with $\tilde{J} = 1.5$, $\tilde{K} = 0.1$ and $L = 160$. Top: a kymograph of θ for a single 1D row in the 3D system. Bottom: M_A and M_B as a function of time. (b) Coherence time τ_c as a function of system size. τ_c is defined as the time for which the envelope of the correlation function $C(\tau) \equiv \langle M_A(t)M_A(t+\tau) \rangle_t$ is a factor of e^{-1} from its initial value. Simulation parameters are $\tilde{J} = 1.6$ and $\tilde{K} = 0.1$. (c) M_B as a function of M_A at steady state for the points marked by stars in panel d. (d) Color map of R as a function of \tilde{J} and \tilde{K} for $L = 320$. Red dot is the pitchfork bifurcation. (e) R as a function of \tilde{J} for $\tilde{K} = 0.3$ (dashed line in panel d) shown for different linear system size L . Inset: R vs. L^{-1} for $\tilde{J} = 1.38, 1.40, 1.42, 1.43, 1.45$ from bottom to top on a log-log scale. (f) critical exponents of the 3D non-reciprocal Ising model (NR Ising) for $\tilde{K} = 0.1$ extracted from finite-size scaling analysis along with their standard deviation represented by a semi-transparent red rectangle, and compared with the 3D Ising model and the 3D XY model. (g) Simulation snapshots of the 3D system showing scroll waves and planar waves. Sites in $\uparrow\uparrow$ state are shown in blue while other sites are not shown. System parameters: $\tilde{J} = 2.28$, $\tilde{K} = 0.3$, $L = 80$.

ciillations (different in nature from the homogeneous noisy oscillations close to the Hopf bifurcation) with oscillation period T_{osc} that converges to a finite value as system size increases (Fig 4b). This is further supported by Figs. 2e and 3e (right parts) showing that the \tilde{J} -transition-point between static order and oscillations in finite systems (indicated by a sharp change in the slope of R) increases with size.

To see why non-reciprocity allows droplets to grow, in contrast with the equilibrium Ising model where they tend to shrink, assume first that the system is in the static-order phase, so most spins in both lattices are up [102]. Since the system is static, it can be mapped into two equilibrium Ising models (Fig. 4c) with opposite magnetic fields, with energy $E = -J \sum_{\langle i,j \rangle} \sigma_i \sigma_j - H \sum_i \sigma_i$ where $H \approx K$ for A-spins and $H \approx -K$ for B-spins (see Eq. (2)). While sub-system A is in a stable state in the effective equilibrium system, sub-system B is in a metastable state, as it prefers a state with opposite magnetization. Sub-system B then transitions to its equilibrium stable state by nucleating droplets larger than a critical size ρ_c whose value depends on \tilde{J} and \tilde{K} . [102, 103]. After a droplet has expanded beyond ρ_c , the stable sub-system becomes metastable and nucleates droplets, and so on (Fig. 4c). Crucially, for finite \tilde{J} and \tilde{K} , ρ_c is finite, making the static-order phase unstable in any finite dimension. Note that when the symmetry between the spin species is broken, droplets do not expand at the same velocity, leading to droplet-capture and shrinkage that re-stabilizes the static-order phase (Fig. 4d and Movie 5). This can be achieved, for example, by modifying the inter-species interaction in the selfish energy, Eq. (2), to be $-K_{\alpha\beta} \sigma_i^\alpha \sigma_i^\beta$ where

$K_{AB} = K_+ + K_-$ and $K_{BA} = K_+ - K_-$ (see Ref. [77] for details).

What is the fate of the droplet-induced oscillations regime occurring at high \tilde{J}/\tilde{K} ? In 2D it is unstable due to spirals (Fig. 2). In 3D, it exhibits large structures with out-of-phase regions [77], in contrast with the more homogeneous swap phase occurring at lower \tilde{J}/\tilde{K} as in Fig. 3a. Moreover, in this regime the degree of synchronization in 3D, while clearly decreasing, does not converge with system size (Fig. 3e, $\tilde{J} \gtrsim 2$). It is therefore unclear whether the resulting phase is disordered or oscillating, but the static order can be ruled out (Fig. 1e).

We have found that the only stable phase in 2D and 3D, other than disorder, is the 3D swap phase. This can be traced to the fact that the swap phase spontaneously breaks a continuous symmetry (continuous time-translation invariance) rather than a discrete one [77]. In this case, an analogy with the Mermin-Wagner theorem [104, 105] in the time domain [106–108] suggests that order is destroyed in $d \leq 2$ by the fluctuations of the Goldstone modes associated with the broken continuous time translation invariance, but is possible in $d \geq 3$. In addition, contrary to discrete symmetries, phases with spontaneously broken continuous symmetries do not support well-defined droplet excitations (domain walls are progressively blurred as time evolves) and are therefore stable against droplet growth [47, 60, 77, 109].

We have shown that a non-reciprocal generalization of the 3D Ising model can act as a stable spatially-distributed clock characterized by well-defined critical properties reminiscent of time-crystals [97, 110–116]. While minimalist, this model contains features arising in models of the human brain [67], opinion dynamics [117, 118], spinor BECs [31, 119, 120] and microme-

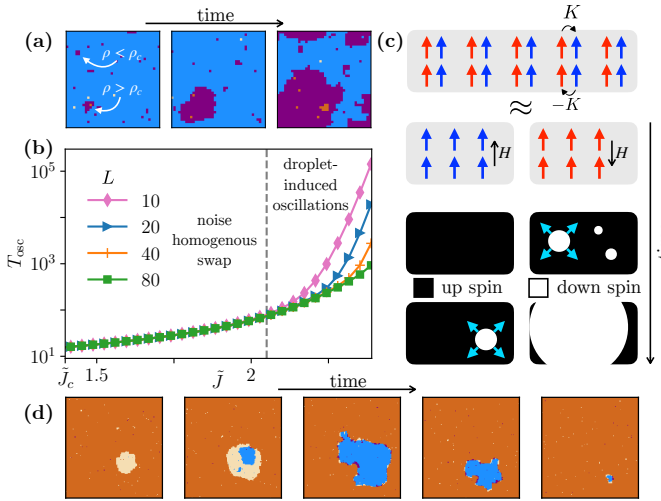


Fig. 4. Fate of static order by droplet growth. (a) Snapshots of the θ field in a 2D system, taken 20 (left) 100 (middle) and 150 (right) MC sweeps after initialization in an ordered state. The largest droplet at $t = 20$ is shown to expand in later times, while the second largest droplet, which did not exceed the critical droplet size, ρ_c , shrunk and disappeared in later times. System parameters: $\tilde{J} = 2.8$, $\tilde{K} = 0.3$, $L = 40$. (b) Oscillation period of the total magnetizations T_{osc} in the 3D system as a function of \tilde{J} for fixed $\tilde{K} = 0.3$. T_{osc} is measured as twice the average time between two subsequent sign flips of M_A . The period is finite at the critical point \tilde{J}_c , supporting a Hopf-like behavior. Dashed grey line separates a regime in which the oscillations are driven by well-defined droplets (right) from a regime in which they do not (left). (c) Schematic drawing of the droplet argument for the instability of the static-order phase. A system in the static-order phase (first row) can be reduced into two equilibrium Ising models subject to magnetic fields (second row), where one system is in a stable equilibrium while the other in a metastable state. The metastable system nucleates droplets that expand and flip the magnetization (third row). The stable system becomes metastable and nucleates droplets that expand with the same velocity (fourth row), and so on. (d) Snapshots of θ in a 2D system for asymmetric non-reciprocity with $\tilde{J} = 3.3$, $\tilde{K}_+ = 0.1$, $\tilde{K}_- = 0.3$, and $L = 150$. Species B nucleates a droplet, but before it reaches system size, a nested droplet of A -spins nucleates and expands at faster speed, eventually catching up with the boundaries of the B -droplet, making it shrink and disappear. This mechanism stabilizes the static-order phase when $\tilde{K}_+ < \tilde{K}_-$ [77].

chanical oscillators [69], which can all be modeled by non-potential spin systems.

ACKNOWLEDGMENTS

We thank G. Biroli, S. Diehl, O. Granek, M. Han, T. Khain, P. Littlewood, R. Mandal, D. Mukamel, S. Sethi, S. Sondhi, G. A. Weiderpass, C. Weiss, and T. Witten for helpful discussions. Y.A., D.S. and M.F. acknowledge support from a MRSEC-funded Kadanoff–Rice fellowship and the University of Chicago Materials Research Science and Engineering Center, which is funded by the National Science Foundation under award no. DMR-2011854. Y.A. acknowledges support from the Zuckerman STEM Leadership Program. D.M., M.F., and V.V. acknowledge support from the France Chicago center through a FACCTS grant. M.F. acknowledges support from the National Science Foundation under grant no. DMR-2118415 and the Simons Foundation. V.V. acknowledges partial support from the Army Research Office under grant nos. W911NF-22-2-0109 and W911NF-23-1-0212 and the Theory in Biology program of the Chan Zuckerberg Initiative. This research was partly supported by the National Science Foundation through the Center for Living Systems (grant no. 2317138) and the National Institute for Theory and Mathematics in Biology (NITMB). All the authors acknowledge the support of the UChicago Research Computing Center which provided the computing resources for this work.

[1] Caleb H. Meredith, Pepijn G. Moerman, Jan Groenewold, Yu-Jen Chiu, Willem K. Kegel, Alfons van Blaaderen, and Lauren D. Zarzar. Predator-prey interactions between droplets driven by non-reciprocal oil exchange. *Nature Chemistry*, 12(12):1136–1142, Nov 2020.

[2] A. V. Ivlev, J. Bartnick, M. Heinen, C.-R. Du, V. Nosenko, and H. Löwen. Statistical mechanics where newton’s third law is broken. *Physical Review X*, 5(1):011035, Mar 2015.

[3] Andrea Cavagna and Irene Giardina. Bird flocks as condensed matter. *Annual Review of Condensed Matter Physics*, 5(1):183–207, Mar 2014.

[4] Lokrshi Prawar Dadhichi, Jitendra Kethapelli, Rahul Chajwa, Sriram Ramaswamy, and Ananya Maitra. Non-mutual torques and the unimportance of motility for long-range order in two-dimensional flocks. *Physical Review E*, 101(5):052601, May 2020.

[5] Élisabeth Guazzelli and John Hinch. Fluctuations and instability in sedimentation. *Annual Review of Fluid Mechanics*, 43(1):97–116, Jan 2011.

[6] Alexander P. Petroff, Xiao-Lun Wu, and Albert Libchaber. Fast-moving bacteria self-organize into active two-dimensional crystals of rotating cells. *Physical Review Letters*, 114(15):158102, Apr 2015.

[7] Tsevi Beatus, Tsvi Tlusty, and Roy Bar-Ziv. Phonons in a one-dimensional microfluidic crystal. *Nature Physics*, 2(11):743–748, Oct 2006.

[8] Curtis W. Peterson, John Parker, Stuart A. Rice, and Norbert F. Scherer. Controlling the dynamics and optical binding of nanoparticle homodimers with transverse phase gradients. *Nano Letters*, 19(2):897–903, Jan 2019.

[9] Dirk Helbing and Péter Molnár. Social force model for pedestrian dynamics. *Physical Review E*, 51(5):4282–4286, May 1995.

[10] Nariya Uchida and Ramin Golestanian. Synchronization and collective dynamics in a carpet of microfluidic rotors. *Physical Review Letters*, 104(17):178103, Apr 2010.

[11] Máté Nagy, Zsuzsa Ákos, Dora Biro, and Tamás Vicsek. Hierarchical group dynamics in pigeon flocks. *Nature*, 464(7290):890–893, Apr 2010.

[12] Yuval Yifat, Delphine Coursault, Curtis W. Peterson, John Parker, Ying Bao, Stephen K. Gray, Stuart A. Rice, and Norbert F. Scherer. Reactive optical matter: light-induced motility in electrodynamic asymmetric nanoscale scatterers. *Light: Science and Applications*, 7(1), Dec 2018.

[13] Knut Drescher, Kyriacos C. Leptos, Idan Tuval, Takuji Ishikawa, Timothy J. Pedley, and Raymond E. Goldstein. Dancing volvox: Hydrodynamic bound states of swimming algae. *Physical Review Letters*, 102(16):168101, Apr 2009.

[14] Kevin D. Lafferty, Giulio DeLeo, Cheryl J. Briggs, Andrew P. Dobson, Thilo Gross, and Armand M. Kuris. A general consumer-resource population model. *Science*, 349(6250):854–857, Aug 2015.

[15] Michel Fruchart, Ryo Hanai, Peter B Littlewood, and Vincenzo Vitelli. Non-reciprocal phase transitions. *Nature*, 592(7854):363–369, 2021.

[16] Suroopriya Saha, Jaime Agudo-Canalejo, and Ramin Golestanian. Scalar active mixtures: The nonreciprocal cahn-hilliard model. *Physical Review X*, 10(4):041009, 2020.

[17] Zhihong You, Aparna Baskaran, and M Cristina Marchetti. Nonreciprocity as a generic route to traveling states. *Proceedings of the National Academy of Sciences*, 117(33):19767–19772, 2020.

[18] Tobias Frohoff-Hülsmann and Uwe Thiele. Nonreciprocal cahn-hilliard equations emerging as one of eight universal amplitude equations. *arXiv preprint arXiv:2301.05568*, 2023.

[19] Maoji Liu, Zhanglin Hou, Hiroyuki Kitahata, Linli He, and Shigeyuki Komura. Non-reciprocal phase separations with non-conserved order parameters. *Journal of the Physical Society of Japan*, 92(9):093001, 2023.

[20] Fridtjof Brauns and M Cristina Marchetti. Nonreciprocal pattern formation of conserved fields. *arXiv preprint arXiv:2306.08868*, 2023.

[21] Sarah A M Loos and Sabine H L Klapp. Irreversibility, heat and information flows induced by non-reciprocal interactions. *New Journal of Physics*, 22(12):123051, Dec 2020.

[22] Michel Fruchart, Colin Scheibner, and Vincenzo Vitelli. Odd viscosity and odd elasticity. *Annual Review of Condensed Matter Physics*, 14(1):471–510, Mar 2023.

[23] Haim Sompolinsky and Ido Kanter. Temporal association in asymmetric neural networks. *Physical review letters*, 57(22):2861, 1986.

[24] B Derrida, E Gardner, and A Zippelius. An exactly solvable asymmetric neural network model. *Europhysics Letters (EPL)*, 4(2):167–173, Jul 1987.

[25] G Parisi. *Journal of Physics A: Mathematical and General*, 19(11):L675–L680, Aug 1986.

[26] Hyunsuk Hong and Steven H Strogatz. Kuramoto model of coupled oscillators with positive and negative coupling parameters: An example of conformist and contrarian oscillators. *Physical Review Letters*, 106(5):054102, 2011.

[27] Hyunsuk Hong and Steven H Strogatz. Conformists and contrarians in a kuramota model with identical natural frequencies. *Physical Review E*, 84(4):046202, 2011.

[28] Valentina Ros, Felix Roy, Giulio Biroli, Guy Bunin, and Ari M Turner. Generalized lotka-volterra equations with random, nonreciprocal interactions: The typical number of equilibria. *Physical Review Letters*, 130(25):257401, 2023.

[29] Jordi Bascompte, Pedro Jordano, and Jens M. Olesen. Asymmetric coevolutionary networks facilitate biodiversity maintenance. *Science*, 312(5772):431–433, Apr 2006.

[30] Michel Loreau and Claire de Mazancourt. Biodiversity and ecosystem stability: a synthesis of underlying mechanisms. *Ecology Letters*, 16(s1):106–115, Jan 2013.

[31] Ezequiel I. Rodríguez Chiacchio, Andreas Nunnenkamp, and Matteo Brunelli. Nonreciprocal dicke model. *Physical Review Letters*, 131(11):113602, Sep 2023.

[32] A. Metelmann and A. A. Clerk. Nonreciprocal photon transmission and amplification via reservoir engineering. *Physical Review X*, 5(2):021025, Jun 2015.

[33] Aashish Clerk. Introduction to quantum non-reciprocal interactions: from non-hermitian hamiltonians to quantum master equations and quantum feedforward schemes. *SciPost Physics Lecture Notes*, Mar 2022.

[34] Clara del Junco and Suriyanarayanan Vaikuntanathan. Robust oscillations in multi-cyclic markov state models of biochemical clocks. *The Journal of Chemical Physics*, 152(5), Feb 2020.

[35] Clara del Junco and Suriyanarayanan Vaikuntanathan. High chemical affinity increases the robustness of biochemical oscillations. *Physical Review E*, 101(1):012410, Jan 2020.

[36] Yuansheng Cao, Hongli Wang, Qi Ouyang, and Yuhai Tu. The free-energy cost of accurate biochemical oscillations. *Nature Physics*, 11(9):772–778, Jul 2015.

[37] Andre C. Barato and Udo Seifert. Coherence of biochemical oscillations is bounded by driving force and network topology. *Physical Review E*, 95(6):062409, Jun 2017.

[38] Chenyi Fei, Yuansheng Cao, Qi Ouyang, and Yuhai Tu. Design principles for enhancing phase sensitivity and suppressing phase fluctuations simultaneously in biochemical oscillatory systems. *Nature Communications*, 9(1), Apr 2018.

[39] Harmen Wierenga, Pieter Rein ten Wolde, and Nils B. Becker. Quantifying fluctuations in reversible enzymatic cycles and clocks. *Physical Review E*, 97(4):042404, Apr 2018.

[40] Basile Nguyen, Udo Seifert, and Andre C. Barato. Phase

transition in thermodynamically consistent biochemical oscillators. *The Journal of Chemical Physics*, 149(4), Jul 2018.

[41] Robert Marsland, Wenping Cui, and Jordan M. Horowitz. The thermodynamic uncertainty relation in biochemical oscillations. *Journal of The Royal Society Interface*, 16(154):20190098, May 2019.

[42] Naoto Shiraishi. Entropy production limits all fluctuation oscillations. *Physical Review E*, 108(4):l042103, October 2023.

[43] Naruo Ohga, Sosuke Ito, and Artemy Kolchinsky. Thermodynamic bound on the asymmetry of cross-correlations. *Physical Review Letters*, 131(7):077101, August 2023.

[44] Lukas Oberreiter, Udo Seifert, and Andre C. Barato. Universal minimal cost of coherent biochemical oscillations. *Physical Review E*, 106(1):014106, July 2022.

[45] Juan A Acebrón, Luis L Bonilla, Conrad J Pérez Vicente, Félix Ritort, and Renato Spigler. The kuramoto model: A simple paradigm for synchronization phenomena. *Reviews of modern physics*, 77(1):137, 2005.

[46] Charles H Bennett, G Grinstein, Yu He, C Jayaprakash, and David Mukamel. Stability of temporally periodic states of classical many-body systems. *Physical Review A*, 41(4):1932, 1990.

[47] G Grinstein, David Mukamel, R Seidin, and Charles H Bennett. Temporally periodic phases and kinetic roughening. *Physical review letters*, 70(23):3607, 1993.

[48] Hugues Chaté, G. Grinstein, and Lei-Han Tang. Long-range correlations in systems with coherent (quasi)periodic oscillations. *Physical Review Letters*, 74(6):912–915, Feb 1995.

[49] Leonardo Brunnet, Hugues Chaté, and Paul Manneville. Long-range order with local chaos in lattices of diffusively coupled odes. *Physica D: Nonlinear Phenomena*, 78(3–4):141–154, Nov 1994.

[50] J.A.C. Gallas, P. Grassberger, H.J. Herrmann, and P. Ueberholz. Noisy collective behaviour in deterministic cellular automata. *Physica A: Statistical Mechanics and its Applications*, 180(1–2):19–41, Jan 1992.

[51] J Hemmingsson and H. J Herrmann. On oscillations in cellular automata. *Europhysics Letters (EPL)*, 23(1):15–19, Jul 1993.

[52] G. Grinstein. Stability of nonstationary states of classical, many-body dynamical systems. *Journal of Statistical Physics*, 51(5–6):803–815, Jun 1988.

[53] Tomas Bohr, G. Grinstein, Yu He, and C. Jayaprakash. Coherence, chaos, and broken symmetry in classical, many-body dynamical systems. *Physical Review Letters*, 58(21):2155–2158, May 1987.

[54] P.-M. Binder and V. Privman. Second-order dynamics in the collective temporal evolution of complex systems. *Physical Review Letters*, 68(26):3830–3833, Jun 1992.

[55] Anaël Lemaître, Hugues Chaté, and Paul Manneville. Cluster expansion for collective behavior in discrete-space dynamical systems. *Physical Review Letters*, 77(3):486–489, Jul 1996.

[56] H Chaté and P Manneville. Evidence of collective behaviour in cellular automata. *Europhysics Letters (EPL)*, 14(5):409–413, Mar 1991.

[57] H. Chate and P. Manneville. Collective behaviors in spatially extended systems with local interactions and synchronous updating. *Progress of Theoretical Physics*, 87(1):1–60, Jan 1992.

[58] Hugues Chaté and Jérôme Losson. Non-trivial collective behavior in coupled map lattices: A transfer operator perspective. *Physica D: Nonlinear Phenomena*, 103(1–4):51–72, Apr 1997.

[59] Jérôme Losson and Michael C. Mackey. Statistical cycling in coupled map lattices. *Physical Review E*, 50(2):843–856, Aug 1994.

[60] G. Grinstein, C. Jayaprakash, and C. H. Bennett. Comment on “second-order dynamics in the collective temporal evolution of complex systems”. *Physical Review Letters*, 73(22):3038–3038, Nov 1994.

[61] Jacek Wendykier, Adam Lipowski, and António Luis Ferreira. Coexistence and critical behavior in a lattice model of competing species. *Physical Review E*, 83(3):031904, Mar 2011.

[62] P.-M. Binder and Juan F. Jaramillo. Stabilization of coherent oscillations in spatially extended dynamical systems. *Physical Review E*, 56(2):2276–2278, Aug 1997.

[63] Kevin Wood, C Van den Broeck, R Kawai, and Katja Lindenberg. Universality of synchrony: critical behavior in a discrete model of stochastic phase-coupled oscillators. *Physical review letters*, 96(14):145701, 2006.

[64] Kevin Wood, C Van den Broeck, R Kawai, and Katja Lindenberg. Critical behavior and synchronization of discrete stochastic phase-coupled oscillators. *Physical Review E*, 74(3):031113, 2006.

[65] Roy J Glauber. Time-dependent statistics of the ising model. *Journal of mathematical physics*, 4(2):294–307, 1963.

[66] J-C Walter and GT Barkema. An introduction to monte carlo methods. *Physica A: Statistical Mechanics and its Applications*, 418:78–87, 2015.

[67] Christopher W Lynn, Eli J Cornblath, Lia Papadopoulos, Maxwell A Bertolero, and Danielle S Bassett. Broken detailed balance and entropy production in the human brain. *Proceedings of the National Academy of Sciences*, 118(47):e2109889118, 2021.

[68] Bernardo A. Mello and Yuhai Tu. Quantitative modeling of sensitivity in bacterial chemotaxis: The role of coupling among different chemoreceptor species. *Proceedings of the National Academy of Sciences*, 100(14):8223–8228, Jun 2003.

[69] C Han, M Wang, B Zhang, MI Dykman, and HB Chan. Controlled asymmetric ising model implemented with parametric micromechanical oscillators. *arXiv preprint arXiv:2309.04281*, 2023.

[70] Sarah A. M. Loos, Sabine H. L. Klapp, and Thomas Martyne. Long-range order and directional defect propagation in the nonreciprocal xy model with vision cone interactions. *Physical Review Letters*, 130(19):198301, May 2023.

[71] Laura Guislain and Eric Bertin. Nonequilibrium phase transition to temporal oscillations in mean-field spin models. *Physical Review Letters*, 130(20):207102, 2023.

[72] Laura Guislain and Eric Bertin. Discontinuous phase transition from ferromagnetic to oscillating states in a nonequilibrium mean-field spin model. *arXiv preprint arXiv:2310.13488*, 2023.

[73] F.W.S. Lima and D. Stauffer. Ising model simulation in directed lattices and networks. *Physica A: Statistical Mechanics and its Applications*, 359:423–429, jan 2006.

[74] Alejandro Sánchez, Juan López, and Miguel Rodríguez. Nonequilibrium phase transitions in directed small-world networks. *Physical Review Letters*, 88(4):048701,

jan 2002.

[75] Adam Lipowski, António Luis Ferreira, Dorota Lipowska, and Krzysztof Gontarek. Phase transitions in ising models on directed networks. *Physical Review E*, 92(5):052811, nov 2015.

[76] Jerome Garnier-Brun, Michael Benzaquen, and Jean-Philippe Bouchaud. Unlearnable games and “satisficing” decisions: A simple model for a complex world. *Physical Review X*, 14(2):021039, 2024.

[77] Yael Avni, Michel Fruchart, David Martin, Daniel Seara, and Vincenzo Vitelli. (to be published).

[78] Steven H. Strogatz. *Nonlinear Dynamics and Chaos*. CRC Press, 2018.

[79] Eugene M. Izhikevich. *Dynamical Systems In Neuroscience*. MIT Press, 2007.

[80] The sign of the phase space angular momentum \mathcal{L} in Eq. (5) is chosen such that it is positive when K is positive. \mathcal{L} is related to the entropy production [121] close to the Hopf bifurcation.

[81] Igor S Aranson and Lorenz Kramer. The world of the complex ginzburg-landau equation. *Reviews of modern physics*, 74(1):99, 2002.

[82] Igor S Aranson, Hugues Chaté, and Lei-Han Tang. Spiral motion in a noisy complex ginzburg-landau equation. *Physical review letters*, 80(12):2646, 1998.

[83] Igor S. Aranson, Lorenz Kramer, and Andreas Weber. Theory of interaction and bound states of spiral waves in oscillatory media. *Physical Review E*, 47(5):3231–3241, May 1993.

[84] Ehud Altman, Lukas M Sieberer, Leiming Chen, Sebastian Diehl, and John Toner. Two-dimensional superfluidity of exciton polaritons requires strong anisotropy. *Physical Review X*, 5(1):011017, 2015.

[85] Gideon Wachtel, LM Sieberer, S Diehl, and Ehud Altman. Electrodynamic duality and vortex unbinding in driven-dissipative condensates. *Physical Review B*, 94(10):104520, 2016.

[86] Hugues Chaté and Paul Manneville. Phase diagram of the two-dimensional complex ginzburg-landau equation. *Physica A: Statistical Mechanics and its Applications*, 224(1-2):348–368, 1996.

[87] Tzer Han Tan, Jinghui Liu, Pearson W Miller, Melis Tekant, Jörn Dunkel, and Nikta Fakhri. Topological turbulence in the membrane of a living cell. *Nature Physics*, 16(6):657–662, 2020.

[88] Jinghui Liu, Jan F Totz, Pearson W Miller, Alasdair D Hastewell, Yu-Chen Chao, Jörn Dunkel, and Nikta Fakhri. Topological braiding and virtual particles on the cell membrane. *Proceedings of the National Academy of Sciences*, 118(34):e2104191118, 2021.

[89] Ani Michaud, Marcin Leda, Zachary T. Swider, Songeun Kim, Jiaye He, Jennifer Landino, Jenna R. Valley, Jan Huisken, Andrew B. Goryachev, George von Dassow, and William M. Bement. A versatile cortical pattern-forming circuit based on rho, f-actin, ect2, and rga-3/4. *Journal of Cell Biology*, 221(8), Jun 2022.

[90] Fridtjof Brauns, Grzegorz Pawlik, Jacob Halatek, Jacob Kerssemakers, Erwin Frey, and Cees Dekker. Bulk-surface coupling identifies the mechanistic connection between min-protein patterns in vivo and in vitro. *Nature Communications*, 12(1), Jun 2021.

[91] Lukas Oberreiter, Udo Seifert, and Andre C Barato. Stochastic discrete time crystals: Entropy production and subharmonic synchronization. *Physical Review Letters*, 126(2):020603, 2021.

[92] Yoshiki Kuramoto and Yoshiki Kuramoto. *Chemical turbulence*. Springer, 1984.

[93] Thomas Risler, Jacques Prost, and Frank Jülicher. Universal critical behavior of noisy coupled oscillators. *Physical review letters*, 93(17):175702, 2004.

[94] Thomas Risler, Jacques Prost, and Frank Jülicher. Universal critical behavior of noisy coupled oscillators: A renormalization group study. *Physical Review E*, 72(1):016130, 2005.

[95] Andrea Pelissetto and Ettore Vicari. Critical phenomena and renormalization-group theory. *Physics Reports*, 368(6):549–727, 2002.

[96] Massimo Campostrini, Martin Hasenbusch, Andrea Pelissetto, Paolo Rossi, and Ettore Vicari. Critical behavior of the three-dimensional xy universality class. *Physical Review B*, 63(21):214503, 2001.

[97] Arthur T Winfree. *The geometry of biological time*, volume 2. Springer, 1980.

[98] Arthur T. Winfree and Steven H. Strogatz. Organizing centres for three-dimensional chemical waves. *Nature*, 311(5987):611–615, Oct 1984.

[99] A.T. Winfree and S.H. Strogatz. Singular filaments organize chemical waves in three dimensions. *Physica D: Nonlinear Phenomena*, 8(1–2):35–49, Jul 1983.

[100] A.T. Winfree and S.H. Strogatz. Singular filaments organize chemical waves in three dimensions ii. twisted waves. *Physica D: Nonlinear Phenomena*, 9(1–2):65–80, Oct 1983.

[101] A.T. Winfree and S.H. Strogatz. Singular filaments organize chemical waves in three dimensions. *Physica D: Nonlinear Phenomena*, 9(3):333–345, Dec 1983.

[102] Vladimir RV Assis, Mauro Copelli, and Ronald Dickman. An infinite-period phase transition versus nucleation in a stochastic model of collective oscillations. *Journal of Statistical Mechanics: Theory and Experiment*, 2011(09):P09023, 2011.

[103] Per Arne Rikvold, H Tomita, S Miyashita, and Scott W Sides. Metastable lifetimes in a kinetic ising model: dependence on field and system size. *Physical Review E*, 49(6):5080, 1994.

[104] N. D. Mermin and H. Wagner. Absence of ferromagnetism or antiferromagnetism in one- or two-dimensional isotropic heisenberg models. *Physical Review Letters*, 17(22):1133–1136, Nov 1966.

[105] P. C. Hohenberg. Existence of long-range order in one and two dimensions. *Physical Review*, 158(2):383–386, Jun 1967.

[106] Ching-Kit Chan, Tony E Lee, and Sarang Gopalakrishnan. Limit-cycle phase in driven-dissipative spin systems. *Physical Review A*, 91(5):051601, 2015.

[107] Romain Daviet, Carl Philipp Zelle, Achim Rosch, and Sebastian Diehl. Nonequilibrium criticality at the onset of time-crystalline order. *Physical Review Letters*, 132(16):167102, 2024.

[108] Johannes Lang, Michael Buchhold, and Sebastian Diehl. Field theory for the dynamics of the open o(n) model. *Physical Review B*, 109(6):064310, 2024.

[109] Brieuc Benvennen, Omer Granek, Sunghan Ro, Ran Yaacoby, Hugues Chaté, Yariv Kafri, David Mukamel, Alexandre Solon, and Julien Tailleur. Metastability of discrete-symmetry flocks. *Physical review letters*, 131(21):218301, 2023.

[110] Vedika Khemani, Roderich Moessner, and S. L. Sondhi.

A brief history of time crystals, 2019.

[111] Norman Y. Yao, Chetan Nayak, Leon Balents, and Michael P. Zaletel. Classical discrete time crystals. *Nature Physics*, 16(4):438–447, Feb 2020.

[112] Michael P. Zaletel, Mikhail Lukin, Christopher Monroe, Chetan Nayak, Frank Wilczek, and Norman Y. Yao. Colloquium : Quantum and classical discrete time crystals. *Reviews of Modern Physics*, 95(3):031001, Jul 2023.

[113] Krzysztof Sacha and Jakub Zakrzewski. Time crystals: a review. *Reports on Progress in Physics*, 81(1):016401, Nov 2017.

[114] Frank Wilczek. Quantum time crystals. *Physical Review Letters*, 109(16):160401, Oct 2012.

[115] Alfred Shapere and Frank Wilczek. Classical time crystals. *Physical Review Letters*, 109(16):160402, Oct 2012.

[116] Marina Evers and Raphael Wittkowski. An active colloidal system showing parallels to a time crystal. *Physica Scripta*, 2023.

[117] Naoki Masuda. Voter models with contrarian agents. *Physical Review E*, 88(5):052803, 2013.

[118] Claudio Castellano, Santo Fortunato, and Vittorio Loreto. Statistical physics of social dynamics. *Reviews of modern physics*, 81(2):591, 2009.

[119] Berislav Buća and Dieter Jaksch. Dissipation induced nonstationarity in a quantum gas. *Physical Review Letters*, 123(26):260401, December 2019.

[120] Nishant Dogra, Manuele Landini, Katrin Kroeger, Lorenz Hruba, Tobias Donner, and Tilman Esslinger. Dissipation-induced structural instability and chiral dynamics in a quantum gas. *Science*, 366(6472):1496–1499, December 2019.

[121] Daniel S Seara, Benjamin B Machta, and Michael P Murrell. Irreversibility in dynamical phases and transitions. *Nature communications*, 12(1):392, 2021.